Theoretical Study of the Proton Transfer between Water and $[FeH(CO)_4]^-$ in Aqueous Solution and Relevance to the Water-Gas Shift Reaction Catalyzed by Iron Pentacarbonyl in the Condensed Phase

Claudio Amovilli,*,† Franca Maria Floris,† Miquel Solà,‡ and Jacopo Tomasi†

Dipartimento di Chimica e Chimica Industriale, Università di Pisa, Via Risorgimento 35, I-56126 Pisa, Italy, and Institut de Química Computacional, Campus de Montilivi, Universitat de Girona, E-17071 Girona, Spain

Received October 5, 2000

Proton transfer between H_2O and $FeH(CO)_4^-$, the assumed slow step of the water-gas shift reaction catalyzed by $Fe(CO)_5$, has been studied with Hartree−Fock and multiconfiguration CASSCF ab initio methods. The calculations have been performed in vacuo and in water solution at 298 K, simulating the solvent as a polarizable continuum medium. The process in solution has been found to be less endothermic than in the gas phase by about 50 kcal/mol. The valence bond analysis, made on the CASSCF wave function along the reaction path, explains the mechanism in terms of a single structure in which the transferred hydrogen is simultaneously bonded to iron and oxygen with a different polarization depending on the reaction coordinate.

1. Introduction

The proton-transfer reaction

$$[FeH(CO)_4]^- + H_2O \rightarrow FeH_2(CO)_4 + OH^- \quad (1)$$

is the slow step of the water-gas shift reaction (WGSR) catalyzed by $Fe(CO)_5$.[1,2] The WGSR

$$CO + H_2O \rightarrow CO_2 + H_2 \quad (2)$$

is a key process for the production of hydrogen for chemical industry, and so far it has been the object of several investigations addressed to improve the environmental conditions required.[3] The homogeneous catalysis by $Fe(CO)_5$ allows the WGSR to be carried out at considerably lower temperature with water present as a liquid. Experimental data reported by Sunderlin and Squires[4] suggested that the above process (eq 1), largely endothermic in the gas phase, is considerably less endothermic in aqueous solution, owing to the strong solvation of the species OH^-, which is a smaller ion than $[FeH(CO)_4]^-$.

Very recently the mechanism of the WGSR catalyzed by $Fe(CO)_5$ in the gas phase has been analyzed in detail through a quantum-mechanical study published by Torrent, Solà, and Frenking.[5] In this paper the authors used gradient-corrected density functional theory (B3LYP) and the ab initio method coupled-cluster CCSD(T), and their calculations confirmed, for the catalytic cycle, the scheme

$$Fe(CO)_5 + OH^- \rightarrow Fe(CO)_4COOH^-$$

$$Fe(CO)_4COOH^- \rightarrow FeH(CO)_4^- + CO_2$$

$$FeH(CO)_4^- + H_2O \rightarrow FeH_2(CO)_4 + OH^-$$

$$FeH_2(CO)_4 \rightarrow H_2 + Fe(CO)_4$$

$$Fe(CO)_4 + CO \rightarrow Fe(CO)_5 \quad (3)$$

The global process was found to be exothermic by 17.2 kcal/mol at the B3LYP level and 9.7 kcal/mol with CCSD(T), while eq 1 was found to be endothermic by 70.3 kcal/mol at the B3LYP level and by 66.6 kcal/mol with CCSD(T), in good agreement with the experimental values of, respectively, 9.8 kcal/mol[6] and 71.5 kcal/mol.[4]

Most of the energy required to overcome the process (1) is provided by the initial formation of the ion $Fe(CO)_4COOH^-$ from $Fe(CO)_5$ and OH^-, which is a highly exothermic process.

In this paper we analyze the effect of water as solvent on the slow step (1) by means of the polarizable continuum model (PCM)[7] in the version implemented in the GAMESS package for quantum-mechanical calculations.[8] This version of PCM allows calculations, including all the solute−solvent interactions with the ab initio multiconfiguration CASSCF method.[9]

* To whom correspondence should be addressed. E-mail: amovilli@dcci.unipi.it.
† Università di Pisa.
‡ Universitat de Girona.

(1) Kang, H.; Mauldin, C.; Cole, T.; Slegeir, W.; Petit, R. *J. Am. Chem. Soc.* **1977**, *99*, 8323.
(2) Gross, D. C.; Ford, P. C. *Inorg. Chem.* **1982**, *21*, 1704.
(3) See for example: Ford, P. C. *Acc. Chem. Res.* **1981**, *14*, 31 and other references therein.
(4) Sunderlin, L. S.; Squires, R. R. *J. Am. Chem. Soc.* **1993**, *115*, 337.
(5) Torrent, M.; Solà, M.; Frenking, G. *Organometallics* **1999**, *18*, 2801.
(6) King, A. D., Jr.; King, R. B.; Yang, D. B. *J. Am. Chem. Soc.* **1980**, *102*, 1028.
(7) Amovilli, C.; Barone, V.; Cammi, R.; Cancès, E.; Cossi, M.; Mennucci, B.; Pomelli, C. S.; Tomasi, J. *Adv. Quantum Chem.* **1998**, *32*, 227.

10.1021/om000854s CCC: $20.00
Publication on Web 02/24/2001

Table 1. FeH (*x*) and HO (*y*) Distances (Å) Defining the Broken Line Which Approximate the Portion of the Reaction Path Studied in This Paper

x	2.60	2.40	2.20	2.00	1.80	1.65	1.60	1.60
y	1.00	1.00	1.05	1.20	1.40	1.60	1.80	3.00

Our results confirm a considerable lowering of the endothermicity, although, for a final consideration about the energy balance on the WGSR, one needs to complete the PCM study by applying the same procedure to all the other processes of the scheme (3). In this work we have also studied the energy profile for the proton transfer (1) along a reliable reaction coordinate, showing the presence, for the reaction in solution, of a transition state while, in the gas phase, the process proceeds along an energetically ascending walk.

Finally, the CASSCF wave function has been transcribed in a valence bond (VB) formalism[10] and a simple chemical interpretation of the electron distribution rearrangement is given.

In the following sections we show all the details of the present work.

2. Computational Details

To define a reaction coordinate, a portion of the energy surface has been constructed by constraining the motion of the transferred hydrogen on a line connecting the oxygen of water to iron. In such way we have derived a two-dimensional map of the energy in terms of the distance of hydrogen from iron (*x*) and the distance of hydrogen from oxygen (*y*). Each point on the map corresponds to a geometry in which the above distances are fixed and all the other internal coordinates are optimized to the best energy. For this map the calculations have been performed at the B3LYP level on the isolated interacting system, using the same iron effective core potential and the same basis set II of the Torrent, Solà, and Frenking paper.[5] By means of this map we have found a reaction path which starts from the complex of the reactants and results in the dissociated products. Along this walk, as already anticipated, the B3LYP energy is monotonically increasing. In Table 1we show the coordinates on the *x*,*y* plane of the points connected by a broken line that we have used to approximate this reaction path in the portion subsequently studied with aqueous solvation.

Having defined the reaction path and the optimized geometries, to get more accurate results for both the gas phase and solution, we have recomputed the energy using a better basis set without pseudopotential on iron. In ref 5 it is remarked that the basis set II is suitable to reproduce geometries but it is not reliable enough to evaluate reaction energies, owing to the lack of diffuse functions. Moreover, the elimination of the pseudopotential on iron, which might be responsible for geometry-dependent superposition errors in the presence of diffuse functions on the other centers, involves a further enlargement of the basis set. For our purposes we have then preferred to prepare an appropriate basis set.

In the proton transfer (1) the CO ligands do not significantly change their charge distribution; therefore, a minimal basis set has been used for these fragments. To reproduce the CO ligand field, this minimal set has been obtained by contracting a suitably even-tempered Gaussian set on the isolated CO. The exponents and the coefficients of this contraction scheme are given in Table 2. For iron on the other hand, because it is strongly involved in the process (1), the basis set must be flexible enough for the valence shell and good enough for the inner shells. Again, a (14s,9p,6d) even-tempered Gaussian set has been contracted to a [6s,4p,2d] set, now using a Dunning-like scheme[11] applied to iron in the state ^{5}D. In Table 3 the details of the iron basis are reported. Finally, for hydrogen and water a standard 6-311G basis set has been used with the addition of p and d Gaussian polarization functions having the exponent 0.8.

The solvent water has been characterized by its macroscopic properties at 298 K, the temperature at which we have studied the reaction, and treated as a continuum polarizable medium. The cavity radii for the system $[(CO)_4HFe\cdots H\cdots OH]^-$ have been fixed for all atoms except for the transferred proton, for which we assumed a dependence on the electronic Mulliken charge. More precisely, the radii are as follows: 1.6 Å for Fe, 1.2 Å for H bonded to Fe, 1.0 Å for H bonded to O, 1.5 Å for O in H_2O, 1.6 Å for O in CO, and 1.8 Å for C. For the transferred H the radius goes from 1.0 to 1.2 Å and clearly it takes intermediate values along the reaction coordinate. For

Table 2. Gaussian Contraction Scheme Used for CO in This Work

C set			O set		
type	exponent	coeff[a]	type	exponent	coeff
s	4500.000	0.001 62	s	8000.000	0.001 77
	1127.712	0.006 42		1950.760	0.007 38
	282.608	0.039 26		475.683	0.046 04
	70.822	0.188 50		115.993	0.228 85
	17.748	0.739 33		28.284	0.886 18
	4.448	1.000 00		6.897	1.000 00
s	4.448	−0.17185	s	6.897	−0.15542
	1.115	0.254 74		1.682	0.409 18
	0.279	1.000 00		0.410	1.000 00
	0.070	−0.06840		0.100	0.097 70
p	20.000	0.020 59	p	40.000	0.022 03
	6.034	0.095 83		8.944	0.180 40
	1.821	0.376 09		2.000	0.802 34
	0.549	1.000 00		0.447	1.000 00
	0.166	0.782 63		0.100	0.208 16
	0.050	−0.03627			

[a] The orbitals are not normalized; 1.0 is in all cases the largest coefficient.

Table 3. Gaussian Contraction Scheme Used for Fe in This Work

type	exponent	coeff[a]	type	exponent	coeff[a]
s	60000.000	0.002 80	p	2000.000	0.002 50
	19050.709	0.006 67		556.512	0.020 03
	6048.826	0.032 71		154.853	0.143 70
	1920.574	0.124 84		43.089	0.699 30
	609.805	0.431 98		11.990	1.000 00
	193.620	1.000 00	p	3.336	0.788 57
	61.477	0.709 13		0.928	1.000 00
s	61.477	−0.23482	p	0.15	1.000 00
	19.520	0.906 45	p	0.05	1.000 00
	6.198	1.000 00	d	100.000	0.007 95
s	6.198	−0.20635		25.119	0.094 05
	1.968	1.000 00		6.310	0.529 76
	0.625	0.577 08		1.585	1.000 00
s	0.625	−0.84431		0.398	0.746 04
	0.198	1.000 00	d	0.100	1.000 00
s	0.063	1.000 00			
s	0.020	1.000 00			

[a] The orbitals are not normalized; 1.0 is in all cases the largest coefficient.

(8) Schmidt, M. W.; Baldridge, K. K.; Boatz, J. A.; Elbert, S. T.; Gordon, M. S.; Jensen, J. H.; Koseki, S.; Matsunaga, N.; Nguyen, K. A.; Su, S. J.; Windus, T. L.; Dupuis, M.; Montgomery, J. A. *J. Comput. Chem.* **1993**, *14*, 1347.

(9) Amovilli, C.; Mennucci, B.; Floris, F. M. *J. Phys. Chem. B* **1998**, *102*, 3023.

(10) Amovilli, C.; Floris, F. M.; Mennucci, B. In *Quantum Systems in Chemistry and Physics*; Hernàndez-Laguna, A, Maruani, J., McWeeny, R., Eds.; Kluwer: Dordrecht, The Netherlands, 2000; Vol. 2, pp 213−231.

(11) Dunning, T. H. *J. Chem. Phys.* **1970**, *53*, 2823.

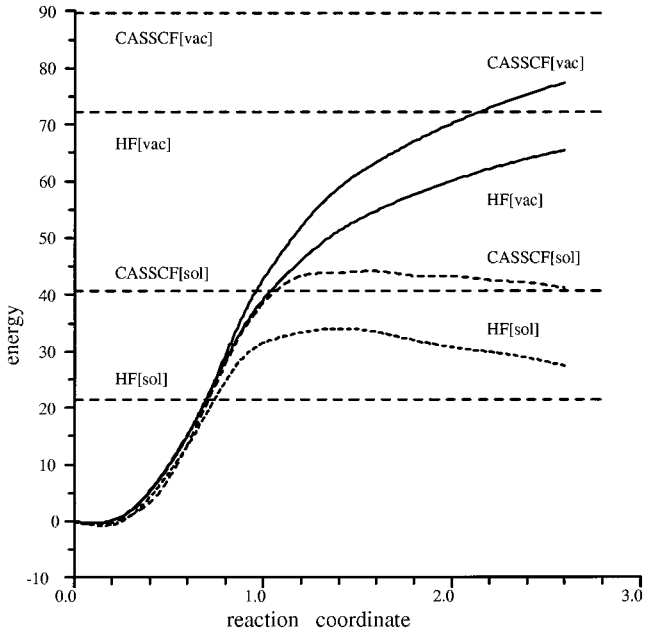

Figure 1. Energy (kcal/mol) in vacuo and free energy in water solution profiles along the reaction coordinate (Å) at the HF and CASSCF levels of calculation. The dashed lines correspond to the energies of the products at infinite separation.

simplicity we have assumed the behavior

$$R = 1.0 + 0.2\left[\frac{q(x,y) - q_0}{q_1 - q_0}\right] \qquad (4)$$

where R is the radius in Å, q_0 is the Mulliken charge of hydrogen in H_2O, q_1 is the Mulliken charge of hydrogen in $FeH_2(CO)_4$, and $q(x,y)$ is the Mulliken charge of the transferred hydrogen along the reaction path.

At this point, having defined all data for the system investigated, we have performed the calculations along the broken line defined in Table 1 at the Hartree−Fock (HF) level and at the CASSCF level, displacing four electrons in four orbitals in the active space. Both kinds of calculations have been done in vacuo and in solution with PCM. Here the PCM includes the ab initio polarization[12] and repulsion and dispersion contributions,[13] while cavitation contribution has been evaluated through the Pierotti−Claverie method.[14,15] The choice of the orbitals for the active space was able to correctly reproduce, for reactants, a lone pair and a diffuse orbital on iron and a bonding and an antibonding orbital between hydrogen and oxygen and, for products, a lone pair and a diffuse orbital on oxygen and a bonding and an antibonding orbital between hydrogen and iron.

3. Results and Discussion

In Figure 1 we show the curves of the energy in vacuo and of the free energy in solution obtained from our calculations along the approximate reaction coordinate defined in Table 1. All energies are referred to the value at the geometry of the reactant complex in vacuo.

The curves in Figure 1 do not include the solute vibrational, rotational, and translational contributions to the free energy; in the PCM these effects are normally assumed to be the same in vacuo and in solution. These contributions to the gas-phase reaction (1) have been estimated in ref 5 and lower the reaction energy by 9 kcal/mol.

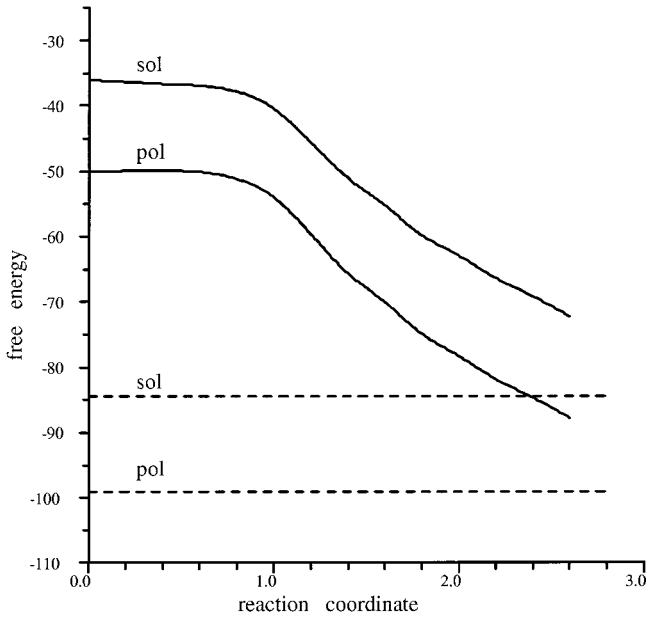

Figure 2. Solvation free energy (kcal/mol) and polarization contribution profiles along the reaction coordinate (Å) as obtained from the CASSCF calculation. The dashed lines correspond to the free energies calculated for the products at infinite separation.

Table 4. Solvation Free Energies and Their Components (kcal/mol) for the Reaction $FeH(CO)_4^-$ + $H_2O \rightarrow FeH_2(CO)_4 + OH^-$ in Water Solution at 298 K as Obtained at the CASSCF Level of Calculation

geom[a]	iec[b]	pol	cav	dis	rep	sol
A	0.5	−55.3	21.4	−13.3	6.3	−40.4
B	0.5	−50.1	20.8	−12.4	5.2	−36.0
C	0.4	−50.0	20.4	−12.4	5.2	−36.4
D	1.3	−70.1	20.6	−11.8	4.8	−55.2
E	0.6	−99.0	21.3	−12.9	5.6	−84.4

[a] Legend: (A) reactants at infinite separation in water; (B) reactant complex in vacuo; (C) reactant complex in water; (D) transition state in water; (E) products at infinite separation in water. [b] Internal energy change.

In Figure 1 an immediate comparison between the CASSCF and HF curves shows that in this case the electron correlation brings about larger reaction energies, the difference being 16.9 kcal/mol in vacuo and 19.4 kcal/mol in water solution. The CASSCF reaction energy in vacuo related to the reactant complex, namely 89.3 kcal/mol, must be compared with the best B3LYP value obtained by Torrent, Solà, and Frenking,[5] which is 82.6 kcal/mol without zero-point and thermal energy corrections. The difference, 7.2 kcal/mol, for this kind of calculation is acceptable; we note that the basis set II of ref 5 gives 115.9 kcal/mol. Moreover, considering the above corrections to the reaction energy, about −5.3 kcal/mol as found in ref 5, and our CASSCF energies for the reactants at infinite separation, we obtain 78.6 kcal/mol, a value comparable also with the experimental estimate of 71.5 kcal/mol.[4]

With regard to the reaction in solution, to our knowledge the present work is the first calculation in the literature.

(12) Cammi, R.; Tomasi, J. *J. Comput. Chem.* **1995**, *16*, 1449.
(13) Amovilli, C.; Mennucci, B. *J. Phys. Chem. B* **1997**, *101*, 1051.
(14) Pierotti, R. A. *Chem. Rev.* **1976**, *76*, 717.
(15) Langlet, J.; Claverie, P.; Caillet, J.; Pullman, A. *J. Phys. Chem.* **1988**, *92*, 1617.

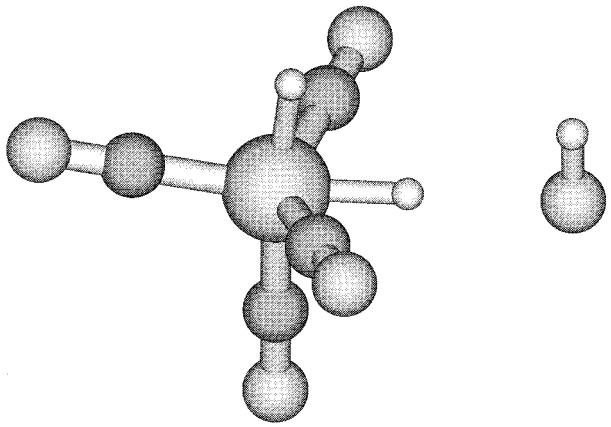

Figure 3. Schematic view of the transition state geometry obtained from the CASSCF study in water solution.

The solvent effect is found to be strong; it reduces the reaction energy from the reactant complex by 48.4 kcal/mol at the CASSCF level and 51.0 kcal/mol at the HF level. These differences correspond to different solvation energies of reactants and products as shown in Figure 2, where the solvation free energy is plotted against the reaction coordinate. In the same figure the polarization contribution is also reported and the comparison of the two curves clearly shows that the solvent effect in this reaction comes essentially from polarization. For completeness in Table 4 we report all solvation data for the CASSCF calculations. With regard to this table, it is important to remark that the dispersion energy is underestimated because of the minimal orbital set used on the CO ligands; nevertheless, this error should be constant along the reaction path. In Table 4 the results for a geometry corresponding to the reactant complex in water are also reported. The total free energy for this configuration is only 0.2 kcal/mol lower than for the geometry corresponding to the same complex in vacuo, and the reactants are slightly more associated. This small effect is simply caused by cavitation.

Finally, the free energy profile in water along the reaction path shows a shallow maximum at both CASSCF and HF levels not present for the in vacuo energy curves (see Figure 1). At these maxima the distances of the transferred proton are 1.60 Å from iron and 2.02 Å from oxygen, while the activation free energy is found to be 44.3 kcal/mol at the CASSCF level; for the HF level, the two distances are respectively 1.60 and 1.82 Å while the activation free energy is 35.3 kcal/mol.

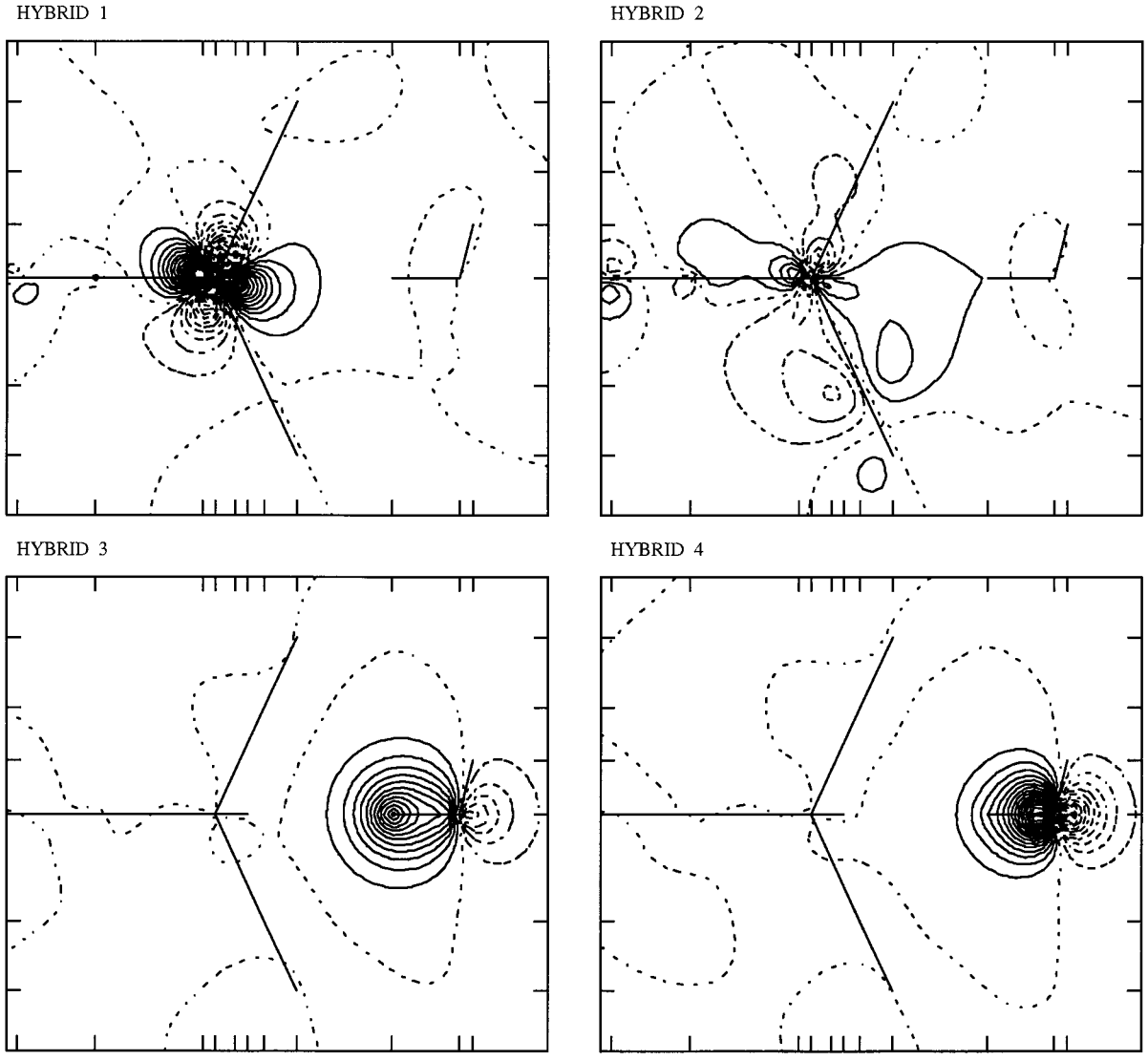

Figure 4. Contour maps of orbitals ϕ_{1-4} for the perfect pairing structure used in the VB analysis for the reactant complex.

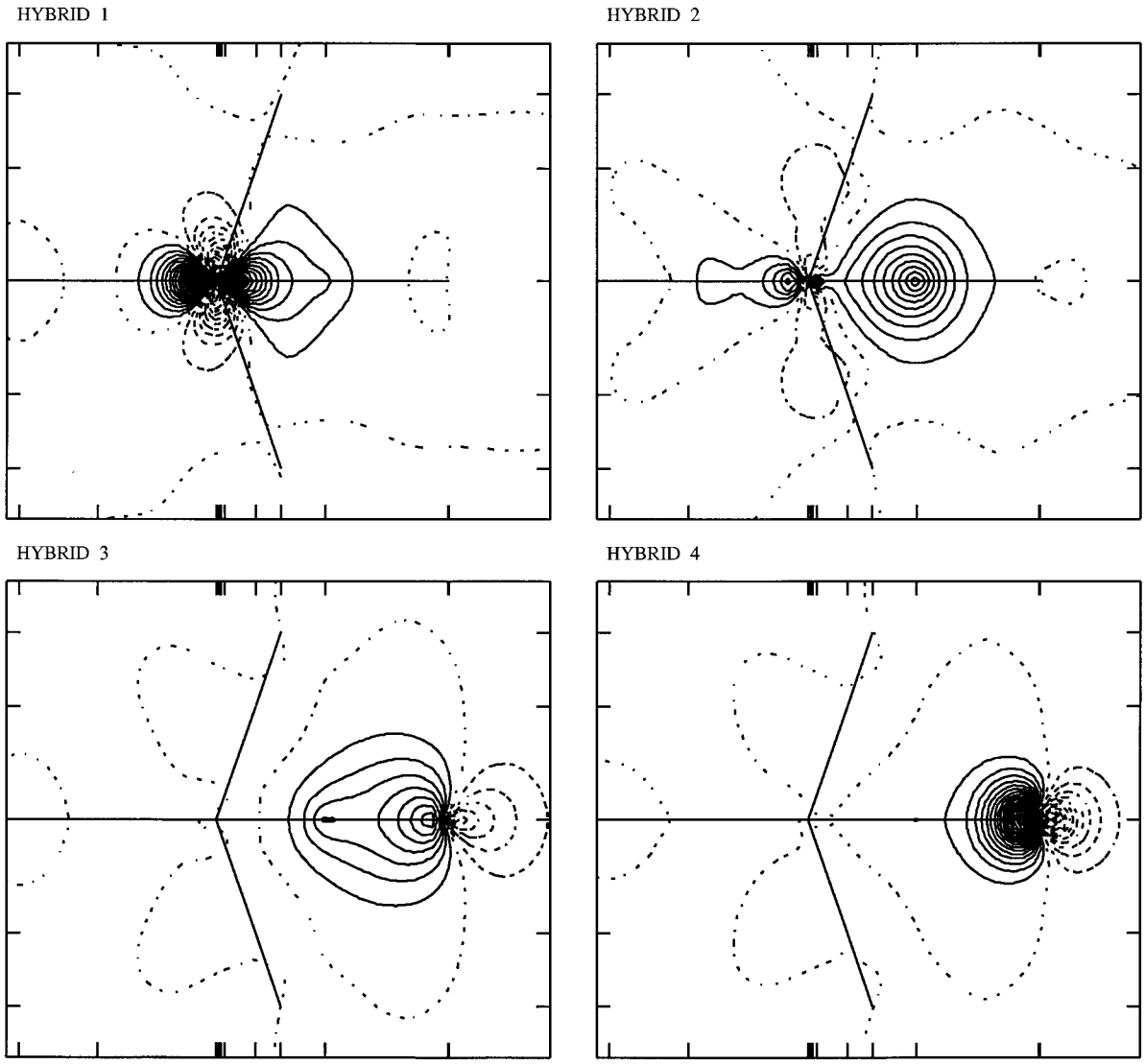

Figure 5. Contour maps of orbitals ϕ_{1-4} for the perfect pairing structure used in the VB analysis in the region of the transition state.

In Figure 3 we show also a schematic view of the system at the transition state as it results from the CASSCF study on the present idealized reaction path. The reader should note that the maximum in the CASSCF curve is only 3.4 kcal/mol higher than the limit of products at infinite separation, and therefore, a better treatment could lead again to a monotonic behavior.

4. Valence Bond Analysis

It is now of some interest to discuss the analysis of the CASSCF wave function along the reaction path in terms of VB structures. As already done in previous papers,[9,10,16] a standard spin-free VB calculation[17] has been attempted in the space spanned by the four active orbitals freezing the MCSCF core. The localization of the active orbitals has been forced by a calculation with one perfect pairing structure. It is important to notice that the best energy for this structure, achieved by mixing the four active CASSCF orbitals, recovers more than 99.8% of the correlation energy of the full-CI space of 20 Weyl−Rumer configurations along the full reaction path. The same result was observed for the S_N2 Menshutkin reaction in water.[9] In this case the electron distribution rearrangement can be represented by a hypervalent hydrogen bonded simultaneously to iron and oxygen with different polarizations depending on the reaction coordinate.

With the notation

$$\Psi_{VB} = K[\hat{A}(\text{core})][\phi_1(1)][\phi_2(2)][\phi_3(3)][\phi_4(4)][\Theta(1,2)][\Theta(3,4)] \quad (5)$$

where

$$\Theta(i,j) = \frac{1}{\sqrt{2}}[[\alpha(i)][\beta(j)] - [\beta(i)][\alpha(j)]] \quad (6)$$

we indicate the perfect pairing structure used to analyze the CASSCF wave function. The ϕ_j values are the optimized generalized hybrids, and they are plotted in Figures 4−6, which correspond respectively to the situations at the reactant complex, in the region of the transition state, and at the dissociation of products. It

(16) Amovilli, C.; Floris, F. M.; Mennucci, B. *Int. J. Quantum Chem.* **1999**, *74*, 59.
(17) McWeeny, R. *Int. J. Quantum Chem.* **1988**, *34*, 25.

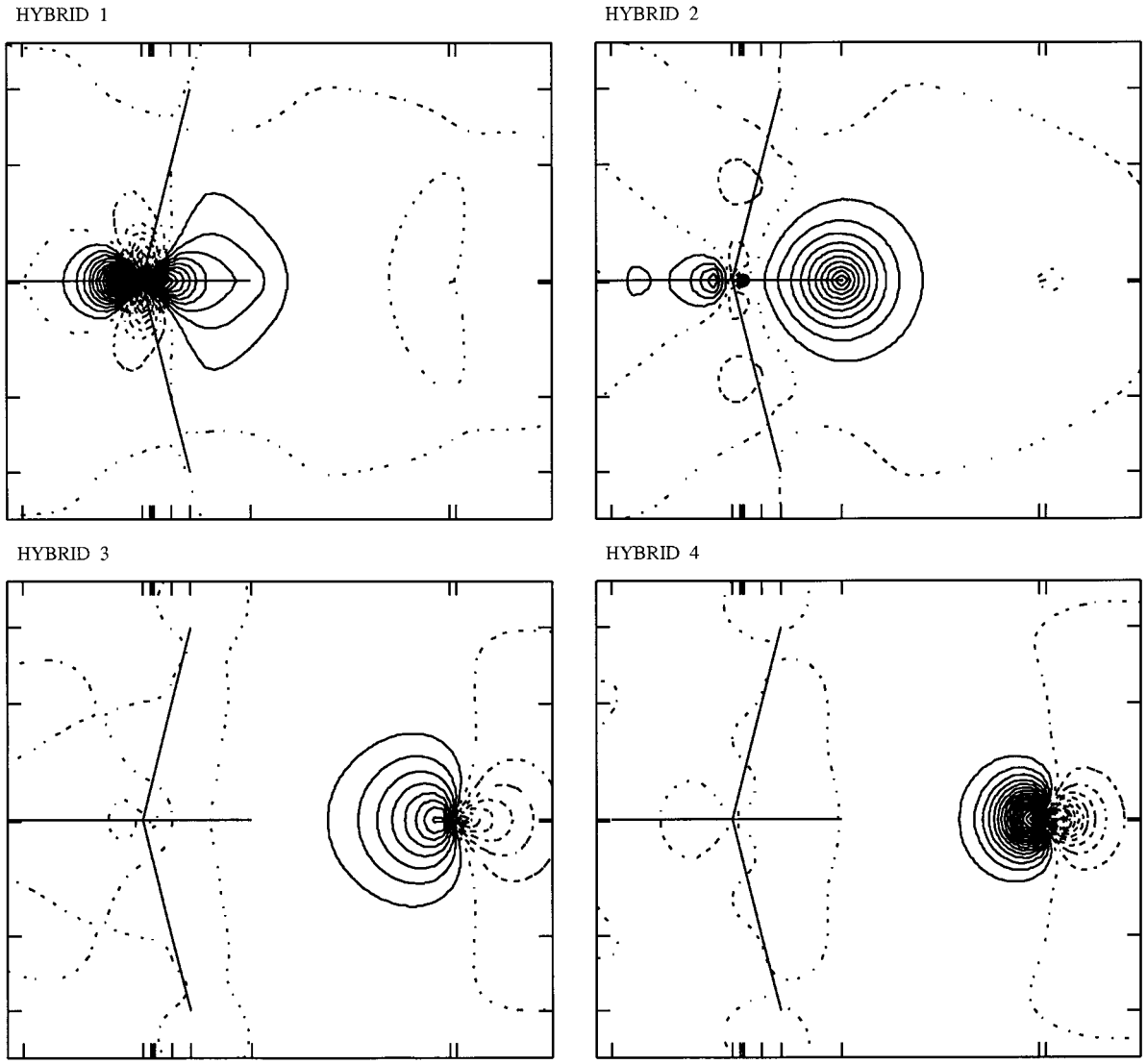

Figure 6. Contour maps of orbitals ϕ_{1-4} for the perfect pairing structure used in the VB analysis at the dissociation of the products.

is evident from Figures 4−6 that in all cases the hybrids ϕ_{1-4} can be written in the form

$$\phi_1 = \chi_{Fe}$$
$$\phi_2 = a\chi'_{Fe} + b\chi_H$$
$$\phi_3 = a'\chi'_O + b'\chi'_H$$
$$\phi_4 = \chi_O \qquad (7)$$

where χ_{Fe}, χ'_{Fe}, χ_H, χ'_H, χ_O, and χ'_O are appropriate localized atomic orbitals and a, a', b, and b' are coefficients which play the role of bond polarization parameters that change along the reaction coordinate. More precisely, along the path

$$\text{reactants} \rightarrow \text{transition state} \rightarrow \text{products}$$

ϕ_2 and ϕ_3 show the modifications

$$\phi_2: \chi'_{Fe} \rightarrow a\chi'_{Fe} + b\chi_H \rightarrow \chi_H$$
$$\phi_3: \lambda\chi'_O + \chi'_H \rightarrow a'\chi'_O + b'\chi'_H \rightarrow \chi'_O \qquad (8)$$

where the mixing coefficients are arranged to give the best overlap with the partner orbitals ϕ_1 and ϕ_4 in the perfect-pairing structure (5) for all the geometries. In modern VB such orbitals are usually called generalized hybrids[18] or overlap enhanced orbitals[17] because they maintain a strong localization but they exhibit tails on the neighbor atoms in order to enhance the covalent character of bonds at the expenses of ionic structures that, consequently, can be discarded. The example of H_2 in the VB treatment given by Coulson and Fischer[19] could be helpful to readers who are not familiar with this kind of argument. Here we remark that, to get four flexible orbitals such as ϕ_{1-4}, a four-electron−four-orbital CASSCF wave function is required.

5. Summary

In this work we present an ab initio study of the proton transfer between water and the ion $[FeH(CO)_4]^-$ in aqueous solution at 298 K. This process is the slow step of the water-gas shift reaction catalyzed by

(18) Cooper, D. L.; Gerratt, J.; Raimondi, M. *Nature* **1986**, *323*, 699.
(19) Coulson, C. A.; Fischer, I. *Philos. Mag.* **1949**, *40*, 306. See also: McWeeny, R. *Coulson's Valence*, 3rd ed.; Oxford University Press: Oxford, U.K., 1979.

$Fe(CO)_5$, and in the gas phase it is an unfavorable process. The study has been performed at the Hartree−Fock level and with the multiconfiguration CASSCF method simulating the solvent by a continuum polarizable medium. The solvent reaction field included polarization, dispersion, and repulsion contributions. The reaction path has been approximated by assuming for the transferred hydrogen a linear motion from oxygen to iron and analyzing a portion of the energy surface obtained for the reaction in vacuo.

The above process has been found to be still endothermic but with a reduction in the reaction energy, starting from the complex of reactants, of about 50 kcal/mol. This strong solvent effect is completely determined by the different polarization contributions to the solvation free energy of reactants and products. This difference arises by the different sizes of OH^- and $[FeH(CO)_4]^-$.

The free energy profile along the reaction coordinate shows a very shallow maximum which instead is not observed for the reaction in the gas phase. The activation energy was found to be 44.3 kcal/mol with CASSCF and 35.3 kcal/mol at the HF level.

Finally we have performed a valence bond analysis projecting the CASSCF wave function onto a perfect pairing structure by mixing the active orbitals. In this way we recovered more than 99.8% of the correlation energy. The electron distribution rearrangement is then interpreted in terms of a hypervalent hydrogen simultaneously bonded to oxygen and iron with different polarizations depending on the reaction coordinate.

Acknowledgment. This work is part of a collaborative project between the University of Pisa and the University of Girona. C.A. and F.M.F. wish to thank Prof. M. Duran for the kind hospitality received during their visit to the Institut de Quìmica Computational in Girona.

OM000854S